# Bioelectrocatalytic Cofactor Regeneration Coupled to CO$_2$ Fixation in a Redox-Active Hydrogel for Stereoselective C−C Bond Formation

*Leonardo Castañeda-Losada, David Adam, Nicole Paczia, Darren Buesen, Fabian Steffler, Volker Sieber, Tobias J. Erb, Michael Richter,\* and Nicolas Plumeré\**

***Abstract:*** *The sustainable capture and conversion of carbon dioxide (CO$_2$) is key to achieving a circular carbon economy. Bioelectrocatalysis, which aims at using renewable energies to power the highly specific, direct transformation of CO$_2$ into value added products, holds promise to achieve this goal. However, the functional integration of CO$_2$-fixing enzymes onto electrode materials for the electrosynthesis of stereochemically complex molecules remains to be demonstrated. Here, we show the electricity-driven regio- and stereoselective incorporation of CO$_2$ into crotonyl-CoA by an NADPH-dependent enzymatic reductive carboxylation. Co-immobilization of a ferredoxin NADP$^+$ reductase and crotonyl-CoA carboxylase/reductase within a 2,2'-viologen-modified hydrogel enabled iterative NADPH recycling and stereoselective formation of (2S)-ethylmalonyl-CoA, a prospective intermediate towards multi-carbon products from CO$_2$, with $92 \pm 6\%$ faradaic efficiency and at a rate of $1.6 \pm 0.4\ \mu mol\,cm^{-2}\,h^{-1}$. This approach paves the way for realizing even more complex bioelectrocatalyic cascades in the future.*

## Introduction

A main goal of carbon capture and utilization technologies is to combine renewable energy with the reduction of CO$_2$ as building block for the synthesis of added-value chemicals, which will allow the transition towards a circular carbon economy. In spite of recent achievements of the electrocatalytic reduction of CO$_2$ into small commodity molecules (CO, methanol, formate, ethylene, among others),[1] the lack of selectivity towards high value-added C$_{2+}$ products[2] has directed attention towards the combination of electrochemistry and biocatalytic steps for CO$_2$ utilization processes.[3,4] Different CO$_2$-transforming enzymes allow access to the fixation of CO$_2$ into a broad range of substrates with high yields and selectivities at mild reaction conditions.[5] The challenge for technical exploitation of this biocatalytic toolbox lies at the interface between electrode and enzyme. Wiring of CO$_2$ reducing enzymes to electrodes is demanding because many of these enzymes require NADPH as natural cofactor for electron transfer.

Targeting the large-scale application of NAD(P)H-dependent oxidoreductases, remarkable progress has been reported on the bioelectrochemical regeneration of the reduced forms of these cofactors. Using direct electron transfer between the electrode and the biocatalyst, Vincent and co-workers reported hydrogen-driven NADH regeneration applied for the stereoselective reduction of ketones and for reductive amination implemented in a flow cell set-up.[6] Similarly, Armstrong and co-workers described the bioelectrochemical regeneration of NADPH, applied to a set of NADPH-dependent enzymatic reactions[7,8] including the fixation of CO$_2$ into pyruvate by malic enzyme.[4]

Using redox-active hydrogels for the immobilization and wiring of the biocatalyst, Minteer and co-workers reported the bioelectrochemical regeneration of NADH, which was applied for the synthesis of polyhydroxybutyrate,[9] methanol and propanol,[10] and more recently chiral β-hydroxy nitriles in a biphasic bioelectrocatalytically driven enzymatic cascade.[11] In comparison to direct electron transfer, the mediated wiring in redox active hydrogels with a high load of enzymes has been shown to enhance the synthetic output of biohybrid systems.[12]

[*] L. Castañeda-Losada, Dr. D. Buesen, Prof. Dr. N. Plumeré
Center for Electrochemical Sciences
Ruhr-Universität Bochum
Universitätsstrasse 150, 44780 Bochum (Germany)

L. Castañeda-Losada, Dr. F. Steffler, Prof. Dr. V. Sieber, Dr. M. Richter
Fraunhofer Institute for Interfacial Engineering and Biotechnology IGB
Schulgasse 11a, 94315 Straubing (Germany)
E-mail: michael.richter@igb.fraunhofer.de

Dr. D. Adam, Dr. N. Paczia, Prof. Dr. T. J. Erb
Department of Biochemistry and Synthetic Metabolism
Max-Planck Institute for Terrestrial Microbiology
Karl-von-Frisch-Strasse 10, 35043 Marburg (Germany)

Dr. D. Buesen, Prof. Dr. V. Sieber, Prof. Dr. N. Plumeré
Technical University Munich, Campus Straubing for Biotechnology and Sustainability
Schulgasse 16, 94315 Straubing (Germany)

E-mail: nicolas.plumere@tum.de

Dr. F. Steffler
Present address: Fraunhofer Center for Chemical-Biotechnological Processes CBP
Am Haupttor (Gate 12, Building 1251), 06237 Leuna (Germany)

Supporting information and the ORCID identification number(s) for the author(s) of this article can be found under:
https://doi.org/10.1002/anie.202103634.

Overall, while NAD(P)H recycling and multistep enzyme reactions, using both direct and mediated electron transfer, have been shown as proof of concept for the synthesis of small molecules that are otherwise inaccessible through electro-catalytic approaches, the direct bioelectrocatalytic $CO_2$ fixation for synthesis of structurally demanding molecules remains to be demonstrated. Here we show that redox-active hydrogel films can be specifically designed to wire and accommodate enzymes for bioelectrocatalytic NADPH regeneration coupled to the synthesis of complex molecules from $CO_2$ via regioselective and stereoselective C−C bond formation. We co-immobilized the enzymes ferredoxin NADP+ reductase (FNR) and NADPH-dependent crotonyl-CoA carboxylase/reductase (Ccr) within a viologen-based redox hydrogel. Electrons transferred to the FNR through a mediated electron transfer mechanism allowed the bioelectrocatalytic reduction of NADP+, thus continuously supplying Ccr with the reduced cofactor to drive the synthesis of (2S)-ethylmalonyl-CoA ($C_{26}H_{42}N_7O_{19}P_3S$, 882 g mol$^{-1}$) by enzymatic reductive carboxylation of crotonyl-CoA.

## Results and Discussion

### Bioelectrocatalytic NADP+ Reduction

Although redox-active hydrogels were previously used for the regeneration of NADH[9,10] their application has not yet been demonstrated for the recycling of NADPH. We use a recently reported 2,2′-viologen modified polyvinyl alcohol (V$^{2+}$-PVA)[13,14] as low-potential redox polymer for the immobilization of FNR from *Synechococcus* sp. directing electrons towards the reduction of NADP+. The biocatalytic film (Figure 1 A), formed by drop casting a mixture of V$^{2+}$-PVA and FNR onto a glassy carbon electrode, was first characterized with cyclic voltammetry (CV). The redox potential of V$^{2+}$-PVA was determined at −466 mV vs. SHE being 110 mV more negative than the standard redox potential of the NADP+/NADPH pair (−355 mV at pH 8[15]) thus providing sufficient driving force for the electron transfer to FNR (Figure 1 B). The stability of the film was tested by performing continuous CVs where over 95 % of the cathodic and anodic peak current densities under non-turnover conditions were kept after 500 cycles corresponding to 1.7 h of continuous cycling (Figure S5A).
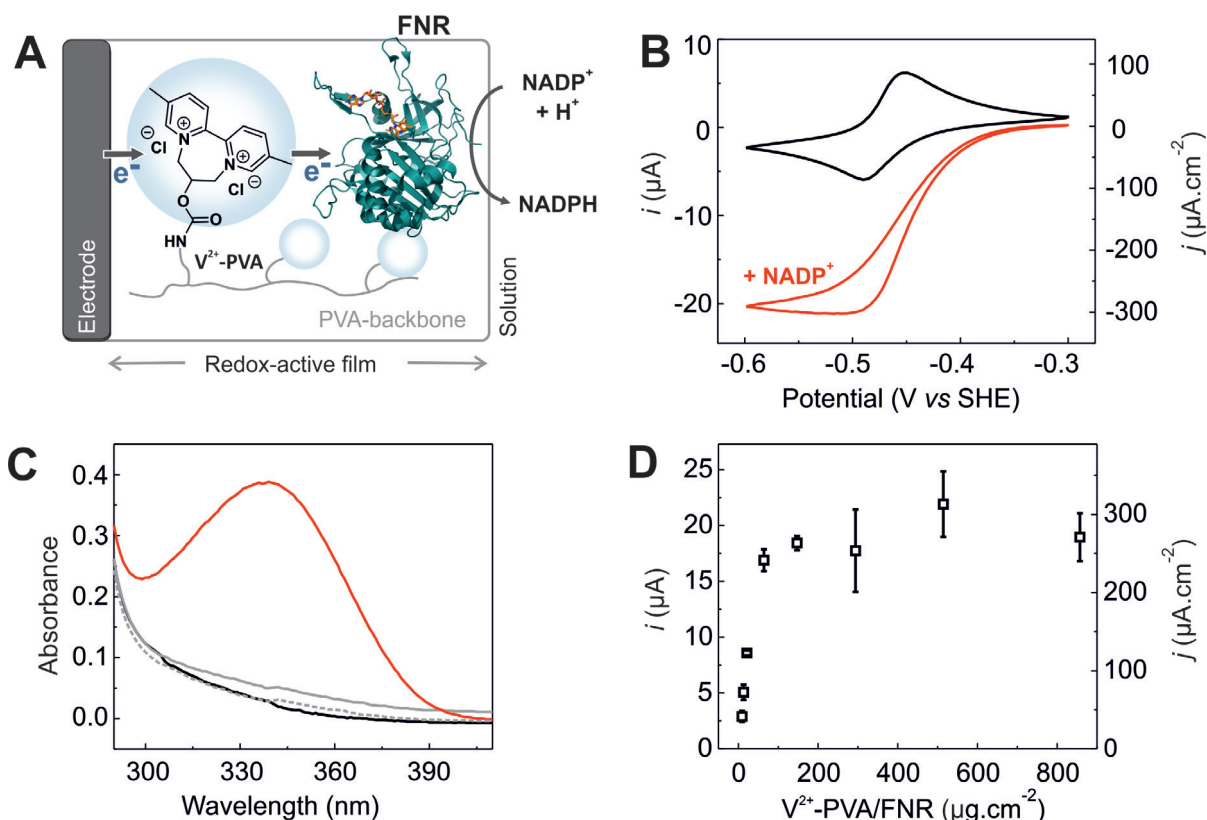


**Figure 1.** Bioelectrocatalytic NADPH generation. A) Schematic representation of NADP+ reduction in films of FNR (PDB 2B5O) immobilized in a viologen-based redox hydrogel (V$^{2+}$-PVA/FNR) on a carbon-based electrode surface. B) Cyclic voltammetry of FNR immobilized within the redox polymer on a glassy carbon electrode (0.07 cm$^2$ area) with V$^{2+}$-PVA/FNR 129/19 µg cm$^{-2}$ in absence (black) and in presence (red) of 9.5 mM NADP+ at 2 mV s$^{-1}$. C) NADPH detection by means of UV/Vis spectroscopy from the electrolyte after bulk electrolysis of V$^{2+}$-PVA/FNR 21/15 µg cm$^{-2}$ on a 1 cm$^2$ Toray paper modified with active and denatured FNR. Background (black), temperature-denatured FNR (dashed gray line), directly deposited FNR (15 µg cm$^{-2}$) without hydrogel (solid gray line), active FNR in the redox active hydrogel (red). D) Catalytic currents for NADP+ reduction as a function of the film thickness (expressed as the amount of deposited polymer and enzyme). All measurements were done with stirring in Tris-HCl (100 mM), KCl (100 mM), pH 8 under argon atmosphere.

The electrocatalytic properties of the modified electrodes are defined by the electroactive film thickness[16] and therefore a uniform film morphology is desired.[17] The electroactive film thickness distribution was quantified using an electroanalytical method based on linear sweep voltammetry.[18] The relative standard deviation in thickness of a thin film of $V^{2+}$-PVA/FNR ($8/1.1 \mu g cm^{-2}$) was 80% (Figure S6) which reflects a significantly higher degree of homogeneity in comparison to previously reported viologen modified polymer films.[17]

In the presence of $NADP^+$, the electrodes modified with $V^{2+}$-PVA/FNR film generate cathodic catalytic current with a half-wave potential ($-442$ mV vs. SHE) near the formal redox potential of the viologen (Figure 1B). This indicates that the viologen moiety mediates the electron transfer between the electrode and the FNR. A maximum in catalytic current of $290 \mu A cm^{-2}$ was obtained for electrodes modified with a ratio of $V^{2+}$-PVA to FNR of $129/19 \mu g cm^{-2}$ in the presence of 9.5 mM $NADP^+$ (Figure 1B). The bioelectrocatalytic $NADP^+$ reduction can also be operated in presence of oxygen (Figure S8 and Table S2). While the rate for NADPH production remained significant, the competing $O_2$ reduction by the redox-active polymer[19–21] strongly decreased the faradaic efficiency. Therefore, the bioelectrocatalyic $NADP^+$ reduction was carried out under inert atmosphere in analogy to previously reported electrochemical NAD(P)H regenerating systems.[10,22–24]

The effect of the film thickness on the catalytic current was tested by modulating the total amount of polymer and enzyme used for electrode modification while maintaining their previously optimized ratio constant[19] (Figure 1D and Figure S5B). The catalytic current for $NADP^+$ reduction increases with polymer and enzyme amount up to a total loading of $60 \mu g cm^{-2}$ and is mostly independent of loading for values above $100 \mu g cm^{-2}$. According to theoretical kinetic models of thin electrocatalytic films[16,25] the initial linear regime can be assigned to current limited by catalyst loading while the thickness-independent currents are due to electron transfer and/or catalysis limitations within the film. For this reason, the maximum bioelectrocatalytic output of the system in terms of both catalytic current and average turnover frequency is reached at the transition between the two regimes at an amount of enzyme and polymer around $100 \mu g cm^{-2}$.

The apparent Michaelis–Menten constant ($K_M$) of $2.4 \pm 0.3$ mM was obtained when fitting the steady-state catalytic current response (at $-595$ mV vs. SHE) to the $NADP^+$ concentration (Figure S22A,B) using the approximate analytical expression for a reaction within a uniform biocatalytic film limited by the substrate amount[16] (see SI 6). The obtained value is two orders of magnitude higher than those reported for other FNRs in solution ($7–30 \mu M$).[15] Substrate depletion within hydrogel films under catalytic turnover is generally the reason for increased values of the apparent Michaelis constant.[26] The $V^{2+}$-PVA/FNR-modified electrode also reduces $NAD^+$ with a similar $K_M$ ($3.6 \pm 0.4$ mM) but at about three-fold lower catalytic currents (Figure S22C,D), highlighting the substrate specificity of the FNR for $NADP^+$.

The bioelectrocatalytic reductive system was further scaled up by drop-casting $V^{2+}$-PVA/FNR onto a Toray paper electrode of $1.0 cm^2$ geometrical area. The film incorporation onto a high-surface-area electrode showed stability comparable to the one on glassy carbon electrodes (Figure S9B). This high film stability was confirmed by monitoring the absorbance of the electrolyte before and after cycling. We detected the absorbance of the polymer corresponding to 22% of the initially deposited amount on the electrode. Most of the lost polymer was released before and early into the cycling, and the remaining polymer (78%) was highly stable as shown by the absence of further loss between 250 and 500 cycles (Figure S9C and Table S3). Addition of $NADP^+$ resulted in an increased cathodic catalytic current (Figure S9A) and generation of NADPH, as demonstrated spectrophotometrically by the appearance of a strong absorbance with a maximum at 340 nm in the UV/Vis spectrum of the bulk of the electrolyte (Figure 1C). In contrast, no catalytic current or NADPH production was detected when FNR was directly deposited on the bare electrode without polymer (Figure S10), when using polymer only (Figure S7A), or when temperature-denatured FNR was immobilized (Figure S7B–E), confirming that the catalytic cofactor reduction takes place via a redox hydrogel-mediated and enzyme-catalyzed process.

At optimal film compositions ($V^{2+}$-PVA/FNR 21/$15 \mu g cm^{-2}$, Figure S9D,E) the NADPH production rate was $1.9 \pm 0.2 \mu mol cm^{-2} h^{-1}$. The turnover frequency (TOF) of the system, calculated as moles of NADPH produced per mole of total amount of FNR per second, was $1.2 \pm 0.1 s^{-1}$ with 10 mM $NADP^+$ at pH 8 (see SI 5). This is three times higher than values obtained with FNR working through a direct electron transfer mechanism when directly immobilized on an ITO electrode ($0.4 s^{-1}$),[15] which highlights the benefits of improved electron transfer to the enzyme when immobilized in the redox hydrogel. The apparent $K_M$ value was $4.4 \pm 0.9$ mM, which was comparable to values achieved with the glassy carbon electrode (Figure S22E,F). The faradaic efficiency of the system was $98 \pm 3\%$, as quantified by the charge consumed during 30 min of electrolysis and the amount of NADPH formed (Figure S11). Taking into account the 220 mV of overpotential used for NADPH formation, we obtain an energy efficiency of 82% for the cathodic half-cell.[27]

To test whether the system was able to fuel NADPH-dependent enzymes, we next coupled glutamate dehydrogenase (GLDH), as well as alcohol dehydrogenase (ADH) to the system after bulk electrolysis. Either enzyme was able to consume the electrochemically formed NADPH to completion (Figure S12), demonstrating that our setup generates the functional NADPH cofactor with high specificity and could be in principle used to operate different NADPH-dependent enzymes.

### CO$_2$ Fixation Coupled to Efficient Bioelectrocatalytic NADPH Regeneration in Redox-Active Hydrogels

Enoyl-CoA carboxylase/reductase (Ecr) enzymes belong to a new class of NADPH-dependent reductive carboxylases which catalyze the stereoselective fixation of CO$_2$ into diverse enoyl-CoAs yielding (2$S$)-alkylmalonyl-CoA as product.[28,29] Members of this family belong to the fastest CO$_2$-fixing enzymes described to date and have been implemented in in vitro and light-powered cyclic multi-enzyme cascades for the continuous fixation of CO$_2$ into organic acids and complex natural products.[30,31] Although these systems have already demonstrated that they provide a promising route for the production of complex chemicals directly from CO$_2$, they are bound to the supply of external chemical energy or to biological energy systems (i.e., photosynthetic membranes).

Thus, an important step towards harnessing the unique capabilities of Ecrs is a setup that would allow to continuously provide these enzymes with reducing equivalents from renewable electricity, which would dramatically expand their application potential ex vivo. To realize this goal, we aimed at coupling the Ecr homologue crotonyl-CoA carboxylase/reductase (Ccr) from *Methylobacterium extorquens* to the developed bioelectrochemical NADP$^+$ reduction platform to continuously incorporate CO$_2$ into crotonyl-CoA (Fig-

ure 2 A). We co-immobilized Ccr on a glassy carbon electrode in the viologen-modified hydrogel (V$^{2+}$PVA/FNR/Ccr) in a 1:1 mass ratio with FNR. CO$_2$ was supplied to the reaction through the addition of HCO$_3^-$ and carbonic anhydrase in the electrolyte. The system was first characterized through cyclic voltammetry.

An increase in catalytic current was observed after the sequential addition of crotonyl-CoA to the electrolyte containing NADP$^+$ and CO$_2$ (Figure 2 B), which was attributed to enhanced local cofactor recycling of the NADP$^+$ formed by Ccr during catalysis. The matching potentials of the redox active polymer and of the catalytic wave indicated a viologen-mediated catalytic process. When temperature-inactivated FNR was immobilized in the film, no catalytic current was observed (Figure S13A,B) and no product was detected, demonstrating that Ccr activity was directly driven by FNR-based NADPH regeneration.

Co-immobilizing enzymes of a multistep catalytic process locally concentrates the biocatalysts in a small volume. The small distances between the catalysts can provide an advantage by allowing the fast diffusive mass transport of intermediates and cofactors between active sites, leading to higher reaction rates[32] and thus enhanced electrocatalytic properties.[7] Such confinement effect was observed when comparing a system with Ccr co-immobilized with FNR in the hydrogel,
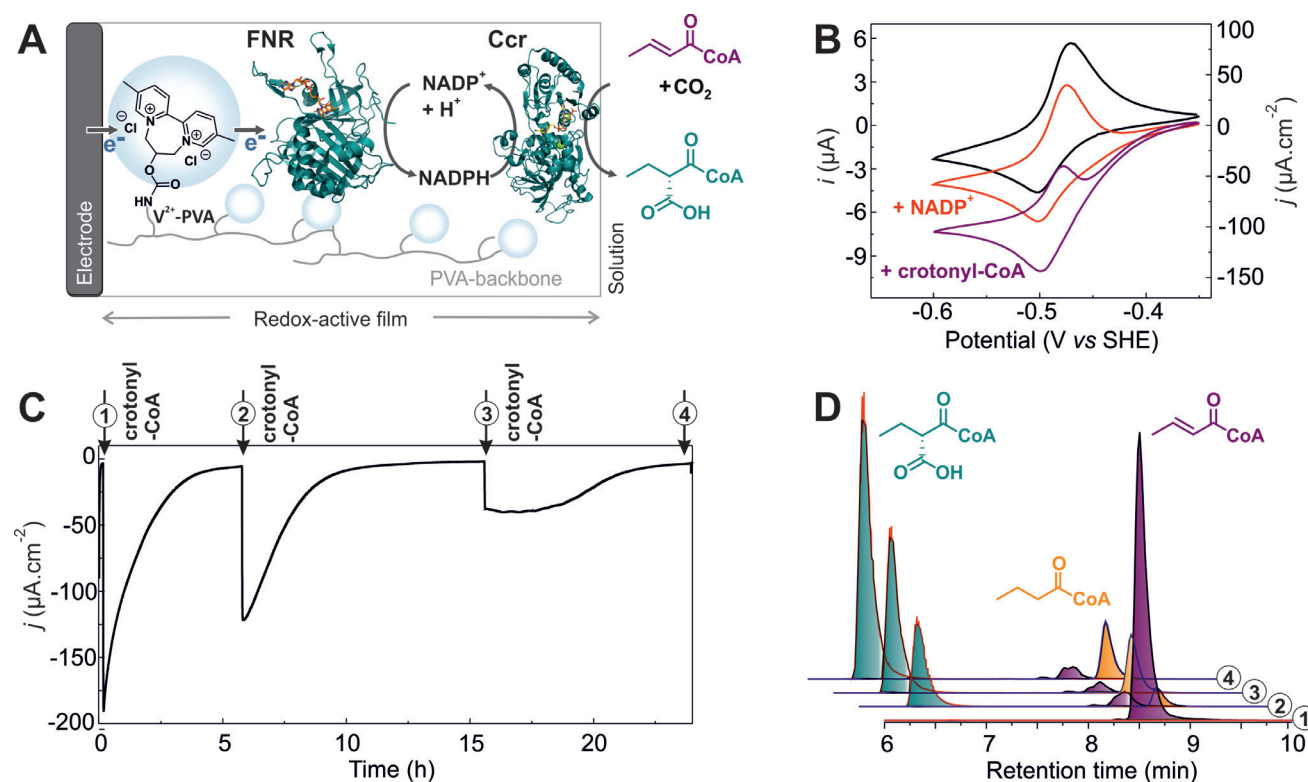


**Figure 2.** Bioelectrocatalytic system for C−C bond formation via reductive carboxylation. A) General scheme for the CO$_2$ incorporation into crotonyl-CoA coupled to bioelectrochemical NADPH regeneration with V$^{2+}$-PVA/FNR/Ccr (PDB 4GI2) 129/19/19 µg cm$^{-2}$ on a glassy carbon electrode (0.07 cm$^2$). B) CVs in absence (black) and presence of 0.2 mM NADP$^+$ (red) and 1.0 mM crotonyl-CoA (purple) at 2 mVs$^{-1}$. C) Long-term CA at −575 mV vs. SHE with three consecutive additions of crotonyl-CoA (1 mM each) in presence of 0.2 mM NADP$^+$. D) Stacked sum of extracted ion chromatograms related to the electrolysis steps from (C). Samples for HPLC–MS analysis were taken prior to each addition of crotonyl-CoA and at the end of the experiment. All experiments were carried out under forming gas in a single compartment cell with 400 µL Tris-HCl (100 mM), KCl (100 mM), pH 8 with NaHCO$_3$ (50 mM) and carbonic anhydrase (1.0 µg mL$^{-1}$).

versus Ccr freely diffusing in solution (Figure S13C,D). In spite of adding a 21-fold higher amount of Ccr when the second enzyme was present freely diffusing in solution, the steady-state catalytic currents were established faster and the absolute values for the catalytic currents were more than double for the co-immobilized Ccr. Confinement also affected overall productivity; while the co-immobilized system showed 30% yield after one hour of electrolysis, only 3% yield was reached with Ccr in solution.

The amount of ethylmalonyl-CoA generated after one hour of electrolysis was used to determine the faradaic efficiency for the $CO_2$ fixation as $92 \pm 6\%$ (Figure S14). Taking into account the 220 mV of overpotential used for (2S)-ethylmalonyl-CoA formation, we obtain an energy efficiency of 77% for the reductive carboxylation (using the $NADP^+/NADPH$ redox potential as reference). A product rate of formation of $1.6 \pm 0.4\ \mu mol\,cm^{-2}\,h^{-1}$ and a TOF of $1.2 \pm 0.3\ s^{-1}$ were calculated for the generation of ethylmalonyl-CoA starting from 1 mM crotonyl-CoA. Using a previously established enzyme assay[33] the stereochemistry of the product was confirmed as (2S)-ethylmalonyl-CoA, while the (2R)-diastereomer was below the detection limit (Figure S15).

Prolonged operation of the system was tested by multiple additions of crotonyl-CoA (Figure 2C). The biocatalytic film maintained substantial activity for over 40 hours of continuous electrolysis, although we observed slow enzyme deactivation or film degradation over the course of the experiment (Figure S17). These experiments also showed that over time the product spectrum was shifted from ethylmalonyl-CoA towards butyryl-CoA, which is formed as side product of Ccr in the absence of $CO_2$, indicating that maintaining constant $HCO_3^-/CO_2$ concentrations in the system is important for long-term operation (Figure S16). Overall, when $HCO_3^-/CO_2$ concentrations were not controlled in the system, the faradaic efficiency for ethylmalonyl-CoA decreased to 55% over the total electrolysis time of 24 h (Figure 2C).

The bioelectrocatalytic system for cofactor regeneration and for reductive carboxylation was optimized for upscaling by screening a wide concentration range of $NADP^+$ (0.01–10 mM) and crotonyl-CoA (0.2–10 mM), respectively (Figure S18). The use of crotonyl-CoA in the low mM range leads to a decrease of one order of magnitude in the apparent $K_M$ for $NADP^+$ (20 μM), adding to the benefits associated with the co-immobilization of the enzymes as a confined cofactor regeneration system. The apparent $K_M$ for crotonyl-CoA is 1.5 mM when using $NADP^+$ at concentrations of 1 mM (Figure S18B).

Aiming to optimize the total turnover number (TTN) for $NADP^+$, we performed full electrolysis in presence of 2 mM crotonyl-CoA (a concentration above the apparent $K_M$) and low $NADP^+$ concentrations (2–200 μM, Figure S19). The unreacted substrate and products were quantified using HPLC–MS after terminating the electrosynthesis (Table S4). In spite of yielding only 12% product, the system could be operated at $NADP^+$ concentrations as low as 2 μM $NADP^+$ leading to a TTN of 117, demonstrating cofactor use at catalytic amounts. Increasing the $NADP^+$ concentration to 20 μM significantly increased the yield to 61% while reaching

a TTN of 61 after 7 hours of reaction. A further increase in the $NADP^+$ concentration up to 200 μM did not strongly impact product yield despite higher reaction rates. Low cofactor concentrations are generally targeted to reach high TTNs and thus for economically competitive cofactor regeneration.[34] When using fragile and complex substrates or products, the total duration of the electrosynthetic process is also an important criterion. In our system, the hydrolysis rate of the substrate (Figure S20), the long-term stability of the film (Figure S17), and the cofactor stability[35,36] impose a maximum reaction time of about one day. This requires high reaction rates that can in principle be achieved with $NADP^+$ concentrations as low as 20 μM without compromising the TTN excessively.

Finally, we scaled up the system into a two-compartment cell (H-Cell with 2 mL volume on the cathode compartment) using a $1.0\ cm^2$ Toray paper electrode (Figure S21) with 4.2 mM of crotonyl-CoA (8.4 μmol, 7 mg). Aiming to secure a maximized conversion of this valuable substrate into ethylmalonyl-CoA, we used 500 μM of the $NADP^+$ cofactor. The reaction was completed after 25 h with an analytical yield of 57% and 91% faradaic efficiency according HPLC–MS. After using preparative HPLC, we obtained the pure product with an overall yield of 37%.

## Conclusion

In this study, we established a bioelectrocatalytic system for NADPH recycling via mediated electron transfer through an immobilized FNR in a viologen-based redox hydrogel of adjusted reduction potential. We showed that the produced NADPH could be further used by co-immobilized Ccr for the reductive fixation of $CO_2$ into crotonyl-CoA. Together, the co-immobilized enzymes constitute an electrically driven cofactor regeneration and coupled $CO_2$ fixation system for stereoselective (2S)-ethylmalonyl-CoA formation at high rates. Our system provides the proof-of-principle for the electro-biocatalyzed $CO_2$-fixation into structurally complex substrates with high regio- and stereocontrol during C—C bond formation. Altogether, the biohybrid system fosters the role of bioelectrochmical $CO_2$ fixation and represents an important step towards synthetic applications of NADPH-dependent enzymes. Further extension of the system through additional enzymes might allow the realization of more complex reaction cascades and pave the way for the development of advanced electrochemically driven synthetic $C_1$ chemistry platforms.

## Acknowledgements

schaft, granted to T.J.E. and V.S. Open access funding enabled and organized by Projekt DEAL.

## Conflict of Interest

The authors declare no conflict of interest.

[1] P. de Luna, C. Hahn, D. Higgins, S. A. Jaffer, T. F. Jaramillo, E. H. Sargent, *Science* **2019**, *364*, eaav3506.

[2] L. Fan, C. Xia, F. Yang, J. Wang, H. Wang, Y. Lu, *Sci. Adv.* **2020**, *6*, eaay3111.

[3] a) K. P. Sokol, W. E. Robinson, A. R. Oliveira, J. Warnan, M. M. Nowaczyk, A. Ruff, I. A. C. Pereira, E. Reisner, *J. Am. Chem. Soc.* **2018**, *140*, 16418; b) M. Yuan, S. Sahin, R. Cai, S. Abdellaoui, D. P. Hickey, S. D. Minteer, R. D. Milton, *Angew. Chem. Int. Ed.* **2018**, *57*, 6582; *Angew. Chem.* **2018**, *130*, 6692; c) S. K. Kuk, K. Gopinath, R. K. Singh, T.-D. Kim, Y. Lee, W. S. Choi, J.-K. Lee, C. B. Park, *ACS Catal.* **2019**, *9*, 5584; d) R. Cai, R. D. Milton, S. Abdellaoui, T. Park, J. Patel, B. Alkotaini, S. D. Minteer, *J. Am. Chem. Soc.* **2018**, *140*, 5041.

[4] G. Morello, B. Siritanaratkul, C. F. Megarity, F. A. Armstrong, *ACS Catal.* **2019**, *9*, 11255.

[5] a) A. Alissandratos, C. J. Easton, *Beilstein J. Org. Chem.* **2015**, *11*, 2370; b) N. Long, J. Lee, K.-K. Koo, P. Luis, M. Lee, *Energies* **2017**, *10*, 473; c) S. Schlager, A. Dibenedetto, M. Aresta, D. H. Apaydin, L. M. Dumitru, H. Neugebauer, N. S. Sariciftci, *Energy Technol.* **2017**, *5*, 812.

[6] a) H. A. Reeve, L. Lauterbach, O. Lenz, K. A. Vincent, *ChemCatChem* **2015**, *7*, 3480; b) C. Zor, H. A. Reeve, J. Quinson, L. A. Thompson, T. H. Lonsdale, F. Dillon, N. Grobert, K. A. Vincent, *Chem. Commun.* **2017**, *53*, 9839.

[7] C. F. Megarity, B. Siritanaratkul, R. S. Heath, L. Wan, G. Morello, S. R. FitzPatrick, R. L. Booth, A. J. Sills, A. W. Robertson, J. H. Warner, et al., *Angew. Chem. Int. Ed.* **2019**, *58*, 4948; *Angew. Chem.* **2019**, *131*, 5002.

[8] G. Morello, C. F. Megarity, F. A. Armstrong, *Nat. Commun.* **2021**, *12*, 340.

[9] B. Alkotaini, S. Abdellaoui, K. Hasan, M. Grattieri, T. Quah, R. Cai, M. Yuan, S. D. Minteer, *ACS Sustainable Chem. Eng.* **2018**, *6*, 4909.

[10] M. Yuan, M. J. Kummer, R. D. Milton, T. Quah, S. D. Minteer, *ACS Catal.* **2019**, *9*, 5486.

[11] F. Dong, H. Chen, C. A. Malapit, M. B. Prater, M. Li, M. Yuan, K. Lim, S. D. Minteer, *J. Am. Chem. Soc.* **2020**, *142*, 8374.

[12] A. Heller, *Curr. Opin. Chem. Biol.* **2006**, *10*, 664.

[13] A. A. Oughli, S. Hardt, O. Rüdiger, J. A. Birrell, N. Plumeré, *Chem. Commun.* **2020**, *56*, 9958.

[14] S. Hardt, S. Stapf, D. T. Filmon, J. A. Birrell, O. Rüdiger, V. Fourmond, C. Léger, N. Plumeré, *Nat. Catal.* **2021**, *4*, 251.

[15] B. Siritanaratkul, C. F. Megarity, T. G. Roberts, T. O. M. Samuels, M. Winkler, J. H. Warner, T. Happe, F. A. Armstrong, *Chem. Sci.* **2017**, *8*, 4579.

[16] P. N. Bartlett, K. F. E. Pratt, *J. Electroanal. Chem.* **1995**, *397*, 61.

[17] H. Li, D. Buesen, R. Williams, J. Henig, S. Stapf, K. Mukherjee, E. Freier, W. Lubitz, M. Winkler, T. Happe, et al., *Chem. Sci.* **2018**, *9*, 7596.

[18] D. Buesen, H. Li, N. Plumeré, *Chem. Sci.* **2020**, *11*, 937.

[19] H. Li, D. Buesen, S. Dementin, C. Léger, V. Fourmond, N. Plumeré, *J. Am. Chem. Soc.* **2019**, *141*, 16734.

[20] H. Li, U. Münchberg, A. A. Oughli, D. Buesen, W. Lubitz, E. Freier, N. Plumeré, *Nat. Commun.* **2020**, *11*, 920.

[21] N. Plumeré, O. Rüdiger, A. A. Oughli, R. Williams, J. Vivekananthan, S. Pöller, W. Schuhmann, W. Lubitz, *Nat. Chem.* **2014**, *6*, 822.

[22] B. Cheng, L. Wan, F. A. Armstrong, *ChemElectroChem* **2020**, *7*, 4672.

[23] X. Zhao, S. E. Cleary, C. Zor, N. Grobert, H. A. Reeve, K. A. Vincent, *Chem* **2021**, *12*, 8105.

[24] H. A. Reeve, L. Lauterbach, P. A. Ash, O. Lenz, K. A. Vincent, *Chem. Commun.* **2012**, *48*, 1589.

[25] C. P. Andrieux, J. M. Dumas-Bouchiat, J. M. Savéant, *J. Electroanal. Chem. Interfacial Electrochem.* **1984**, *169*, 9.

[26] F. Battaglini, E. J. Calvo, *J. Chem. Soc. Faraday Trans.* **1994**, *90*, 987.

[27] R. Küngas, *J. Electrochem. Soc.* **2020**, *167*, 044508.

[28] T. J. Erb, I. A. Berg, V. Brecht, M. Müller, G. Fuchs, B. E. Alber, *Proc. Natl. Acad. Sci. USA* **2007**, *104*, 10631.

[29] D. M. Peter, L. Schada von Borzyskowski, P. Kiefer, P. Christen, J. A. Vorholt, T. J. Erb, *Angew. Chem. Int. Ed.* **2015**, *54*, 13457; *Angew. Chem.* **2015**, *127*, 13659.

[30] T. E. Miller, T. Beneyton, T. Schwander, C. Diehl, M. Girault, R. McLean, T. Chotel, P. Claus, N. S. Cortina, J.-C. Baret, et al., *Science* **2020**, *368*, 649.

[31] T. Schwander, L. Schada von Borzyskowski, S. Burgener, N. S. Cortina, T. J. Erb, *Science* **2016**, *354*, 900.

[32] C. F. Megarity, B. Siritanaratkul, B. Cheng, G. Morello, L. Wan, A. J. Sills, R. S. Heath, N. J. Turner, F. A. Armstrong, *ChemCatChem* **2019**, *11*, 5662.

[33] T. J. Erb, V. Brecht, G. Fuchs, M. Müller, B. E. Alber, *Proc. Natl. Acad. Sci. USA* **2009**, *106*, 8871.

[34] X. Wang, T. Saba, H. H. P. Yiu, R. F. Howe, J. A. Anderson, J. Shi, *Chem* **2017**, *2*, 621.

[35] J. T. Wu, L. H. Wu, J. A. Knight, *Clin. Chem.* **1986**, *32*, 314.

[36] I. Zachos, M. Döring, G. Tafertshofer, R. C. Simon, V. Sieber, *Angew. Chem. Int. Ed.* **2021**, *60*, 14701.